

Tuning Lubrication Performance of Phase-Changing Emulsion-Filled Gels by Sugar Alcohols

Yao Lu, Andrea Araiza-Calahorra, Yanxiang Gao, Like Mao,* and Anwasha Sarkar*

Lubrication by hydrogels is an emerging area in surface science. Although oil-driven friction reduction is predominant in literature, emulsion gel-based lubrication has attracted very little attention to date. We hypothesize that an interplay of viscoelasticity and oil volume fraction may modulate the lubricity of emulsion-filled gels. Herein, phase-change gelatin-based emulsion-filled gels with different sugar alcohols and oil droplet concentrations (0–30 wt%) are tested for their lubrication performance. The rheological and tribological tests are analyzed in conjunction with spectroscopic and structural characterizations to reveal structure–function relationship. Structural characterizations demonstrate that hydrogen bonding is enhanced in pure gelatin gels with the increase of sugar alcohol (glycerol)-replacement time, which enhance the storage modulus (G') of the gel networks. Emulsified droplets serve as active fillers further strengthening the G' and strikingly the presence of glycerol reduced the thermoresponsiveness of the emulsion-filled gels. Emulsion-filled gels containing sugar alcohols, irrespective of their type, can greatly reduce the friction coefficients (μ) between hydrophobic surfaces in the boundary and mixed regimes versus the systems without sugar alcohols. In the hydrodynamic regime, the friction coefficient of the system is proportional to the second plateau shear viscosity, regulated by the oil content.

texture, conducting electricity, and wound healing in food, medicine, and personal care fields.^[2–5] The relationship between microstructure and performance of gel systems is currently a prominent area for research.^[6,7] Of particular interest lately is gel tribology, the science that deals with the lubrication and wear properties of gels between two contact surfaces in relative motion.^[8] The lubricating behavior of gels significantly influences sensory performance (e.g., smoothness or stickiness) in oral and skin surfaces.^[9] In particular, integrating tribological findings with rheological results can provide fundamental insights into the structure–function relationship of gels.^[10]

In particular, lubrication behavior can be affected by elasticity, adhesion, viscosity, hydrophobicity, etc.^[9,11,12] One of the strategies for tuning structure and hence lubricity of gel systems is modification of the continuous phase. Sugar alcohols (also known as polyols), which are highly miscible with water, have been shown to be a

good solvent in which a homogeneous hydrophilic scaffolds can be constructed.^[1,13,14] The polyhydroxy structure of sugar alcohols has been found to be an efficient strategy to achieve low friction *via* hydration lubrication mechanism.^[15] For instance, Li et al. (2015 and 2011) found that mixtures of polyhydroxy lubricants (silicone oil) and acids (sulfuric acid, hydrochloric acid) exhibited superlubricity.^[16,17] This super lubrication mechanism was attributed to the hydrogen bond of polyhydroxy lubricants forming a hydrated lubricating film in the tribocontact region. In addition, it has also been demonstrated that tribostress-mediated degradation of glycerol result in formation of nanometric tribofilms containing organic acids and water and those films can generate ultralow friction.^[18] Therefore, it seems that the polyhydroxyl groups inherent in sugar alcohols holds the potential to introduce novel dimensions to the lubrication properties within gel systems by influencing the structural dynamics of the gel network, which has attracted limited attention to date.


In addition to the continuous phase, another strategy for tuning gel architecture is the filling of oil droplets in the dispersed phase. Our previous study found that emulsified oil droplets stabilized by proteins can act as “active fillers” in the gel network and participate in strengthening a gel network.^[19] It has also been proposed in many studies that the rheological properties and lubrication behavior of emulsion-filled gel systems can be modulated by the volume fraction and size of oil

1. Introduction

Gel systems are a class of soft, swollen materials fabricated using cross-linking polymers in presence of solvent.^[1] Through the design of intricate microstructure, gel systems have widespread applications such as drug delivery systems, modifying food

Y. Lu, Y. Gao, L. Mao
College of Food Science & Nutritional Engineering
China Agricultural University
Beijing 100083, China
E-mail: likemao@cau.edu.cn

Y. Lu, A. Araiza-Calahorra, A. Sarkar
Food Colloids and Bioprocessing Group
School of Food Science and Nutrition
University of Leeds
Leeds LS2 9JT, UK
E-mail: A.Sarkar@leeds.ac.uk

 The ORCID identification number(s) for the author(s) of this article can be found under <https://doi.org/10.1002/adem.202400121>.

© 2024 The Author(s). Advanced Engineering Materials published by Wiley-VCH GmbH. This is an open access article under the terms of the Creative Commons Attribution License, which permits use, distribution and reproduction in any medium, provided the original work is properly cited.

DOI: 10.1002/adem.202400121

droplets, and the interaction between the oil droplets and the matrix networks.^[20–23] Chojnicka et al. (2009) found that the coefficient of friction in the hydrodynamic regime increased with increasing oil concentration for gels containing oil droplets bound to the matrix.^[24] Mu et al. (2022) observed that the friction of casein-stabilized emulsion droplet-filled gels increased with sliding speeds.^[25] This was attributed to oil droplets being released from the disrupted gel structure altering the roughness of the contact interface.^[23] Whilst the effect of filled oil droplets alone on the friction of gel systems has been explored, the relative contribution by the continuous and dispersed phases on frictional dissipation in emulsion-filled gel remains unknown.

Herein, we aimed to understand how structure of phase-changing, emulsion-filled gelatin gels can be regulated by tuning the continuous viscoelastic network (sugar alcohol substitution) or the dispersed phase (oil droplet volume fraction) simultaneously. A combination of low-field nuclear magnetic resonance (LF-NMR) and Fourier transform infrared (FTIR) spectroscopy provided evidence of molecular interactions between gelatin and sugar alcohols (glycerol). We also asked whether the type of sugar alcohols (glycerol, sorbitol, xylitol, and maltitol) affects the lubrication performance of sugar-alcohol-substituted emulsion-filled gelatin gels. Rheology and tribology tests were coupled with microstructural analysis using cryo-scanning electron microscopy (cryo-SEM) and confocal laser scanning microscopy (CLSM) to arrive at structure–function relationship conclusions in these phase-change emulsion-filled gels. We expect that these results will inform the design principles for future engineering of highly lubricating gel materials.

2. Results and Discussion

First, we uncovered the interaction between gelatin-based hydrogels (without added emulsion droplets) and sugar alcohol using glycerol as an exemplar. We then discuss the importance of glycerol in the continuous phase and dispersed phase volume fraction (oil droplet concentration) in the structure and lubricity of emulsion-filled gels and compared how the different types of sugar alcohols, such as sorbitol, xylitol, and maltitol, may affect the lubrication performance of these multicomponent systems.

2.1. Effect of Glycerol on the Properties of Gelatin-Based Hydrogels

Figure 1 systematically compares the structure and properties of gelatin-based hydrogels to elucidate the mechanism of action of glycerol on the gelatin polymer network at different substitution times. In **Figure 1a**, the magnetic resonance imaging (MRI) image of the gelatin hydrogel is presented after pseudo-color treatment. Noticeably, longer glycerol replacement time led to an expanded red region, with a shift in image color from blue to red. In pseudo-color images, red areas typically indicate larger resonance signals and higher hydrogen proton densities.^[26] This suggests that glycerol molecules, with its polyhydroxy structure, enhanced the hydrogen proton density within the gelatin gel system. Comparing the 0.5 and 1 h samples, the red region

gradually entered from the gel's edge to the center, indirectly illustrating the glycerol replacement path.

This variation in hydrogen proton density directly influenced the morphology and network structure of the gel. As shown in **Figure 1b**, the gelatin hydrogel initially appeared as a light-yellow transparent gel with well-defined boundaries. However, as glycerol substitution time increased, the gel's transparency decreased, its color deepened, and volume reduction occurred, displaying a shrinkage phenomenon. Analyzing cryo-SEM micrographs, we attributed this transparency change to a substantial increase in the gel network density induced by glycerol.^[1] The 0 h hydrogel (without glycerol addition) in contrast exhibited a large network pore size, while the 2 h replaced hydrogel displayed nearly no visible voids in the cross-section. This dense and homogeneous network structure reinforced by glycerol altered the gel's color by influencing light reflection, ultimately causing the gel volume to shrink.^[14] To gain deeper insights into the impact of glycerol on altering the pore size of the gel network, we conducted an analysis of the infrared spectra of the hydrogel systems. As illustrated in **Figure 1c**, the initial hydrogel system without glycerol replacement (0-h) exhibits strong peaks corresponding to N–H and O–H stretching vibration at 3308.32 cm^{-1} . The broadness of these peaks indicated the presence of intermolecular hydrogen bonds in the gelatin molecular chain.^[27] Upon introducing glycerol into the gelatin hydrogel systems (0.5–2 h), the absorption peak of the gels underwent a blueshift to lower wavelengths ($3283.67\text{--}3284.46\text{ cm}^{-1}$), which was attributed to the formation of hydrogen bonding between the N–H and O–H groups of the gelatin molecule and the O–H groups of glycerol.^[28] Moreover, the system with glycerol substitution (0.5–2 h) showed absorption peaks around $2944.35\text{--}2934.87\text{ cm}^{-1}$, which corresponded to the asymmetric stretching vibrations of gelatin chains CH and NH.^[27] This suggested that the addition of glycerol also affected the intramolecular interactions within the gelatin molecule. Gelatin hydrogels (0 h) initially displayed an amide I band absorption peak near 1634.97 cm^{-1} caused by stretching of the C=O group.^[29] After glycerol substitution, the wave number corresponding to the amide I band of gelatin increased to $1642.42\text{--}1646.34\text{ cm}^{-1}$, confirming that the addition of glycerol changed the secondary structure of the gelatin protein. Thus, the substitution of glycerol-induced changes in both intra- and intermolecular interactions among the gelatin molecules. The mutual cross-linking between gelatin and glycerol molecules, resulted in the formation of a more compact network structure of the hydrogels, with hydrogen bonding identified as the main driving force to enhance these network structures.

The presence of hydrogen bonding networks in the gel system inevitably influences the distribution and migration of hydrogen protons. LF-NMR, a nondestructive and accurate tool for characterizing hydrogen proton freedom, measures the spin–spin relaxation time (T_2) and aids in the predicting lattice size and distribution within the network.^[30] In **Figure 1d**, the decay curves of the gel systems after the radiofrequency pulse sequence interference reveal an accelerated decay process with an increase in glycerol substitution time. Notably, the 2 h hydrogel displays faster equilibrium, indicating stronger interactions with gelatin macromolecules in the system.^[31]

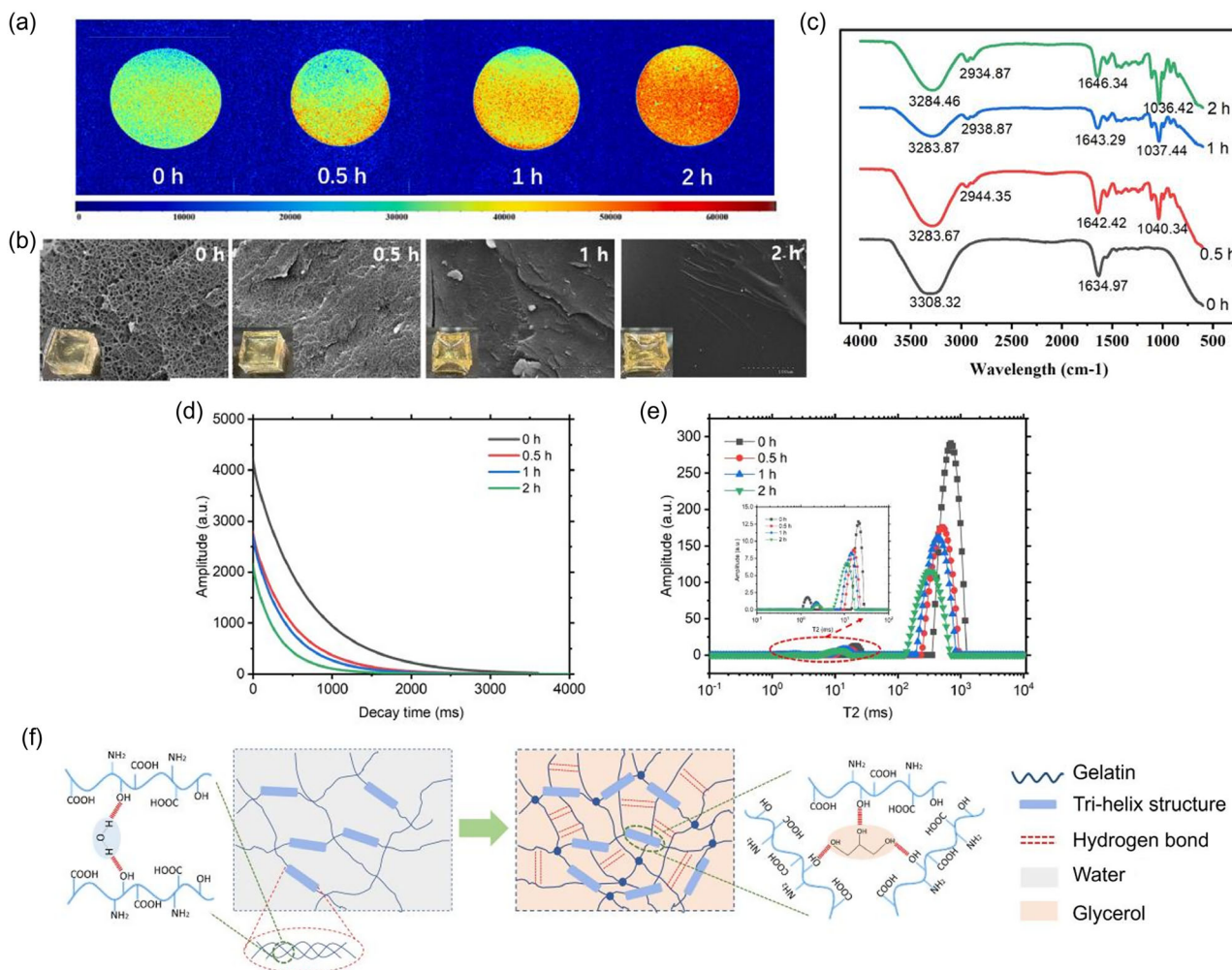


Figure 1. a) Effect of the replacement time of glycerol on the structure of gelatin-based hydrogels evidenced using pseudo-color nuclear magnetic resonance (NMR) images; cryogenic-scanning electron micrographs (cryo-SEM) with insets of b) macroscopic images of the gelatin gels, c) Fourier-transform infrared (FTIR) spectrum, d) relaxation time (T_2) distribution curves obtained from LF-NMR; e) the Carr–Purcell Meiboom–Gill (CPMG) decay curves of T_2 , and f) a schematic diagram of the interactions between gelatin and glycerol. Values are expressed as means and standard deviations of three measurements on triplicate samples ($n = 3 \times 3$).

Table 1. Relaxation time and peak area proportion of gelatin-based hydrogels with different displacement times by sugar alcohol (glycerol). Values are expressed as means and standard deviations of three measurements on triplicate samples ($n = 3 \times 3$). Different subscript lower case letters in the same column indicate a statistically significant difference ($p < 0.05$).

	Time of relaxation [ms]			Proportion of peak area [%]		
	T_{2b}	T_{21}	T_{22}	P_{2b}	P_{21}	P_{22}
0 h	1.431 ± 0.15 ^{a)}	20.491 ± 3.64 ^{a)}	698.588 ± 0.01 ^{a)}	0.266 ± 0.84 ^{b)}	2.253 ± 0.80 ^{b)}	97.482 ± 0.72 ^{b)}
0.5 h	2.274 ± 0.21 ^{a)}	16.268 ± 2.92 ^{a)}	523.110 ± 0.07 ^{a)}	0.209 ± 0.47 ^{b)}	2.876 ± 0.15 ^{b)}	96.915 ± 0.57 ^{b)}
1 h	2.270 ± 0.31 ^{a)}	14.581 ± 4.53 ^{a)}	439.760 ± 0.10 ^{a)}	0.248 ± 0.43 ^{b)}	3.127 ± 0.08 ^{b)}	96.625 ± 0.44 ^{b)}
2 h	2.409 ± 0.17 ^{a)}	11.490 ± 1.54 ^{a)}	329.297 ± 0.15 ^{a)}	0.229 ± 0.65 ^{b)}	3.733 ± 0.33 ^{b)}	96.038 ± 0.36 ^{b)}

^{a)} T_{2b} , T_{21} , and T_{22} represent the relaxation time of free water, intermediate water, and bound water in the gel system, respectively. ^{b)} P_{2b} , P_{21} , and P_{22} represent the proportions of the peaks that are of free water, intermediate water, and bound water in the gel system, respectively.

Figure 1e shows the T_2 distribution peaks obtained from fitting and inversion of the decay curves. All hydrogel systems showed three peaks, namely T_{2b} , T_{21} , and T_{22} , representing

lateral relaxation times of different hydrogen protons states in the gel (Table 1). T_{2b} (0.1–10 ms) corresponds to hydrogen protons closely associated with matrix macromolecules; T_{21}

(10–100 ms) belongs to less mobile hydrogen protons confined by the gel structure; and T_{22} (100–1000 ms) belongs to the free hydrogen protons outside the gel structure.^[32,33] The leftward shift and significant decrease in the peak value of T_{22} with increasing glycerol substitution time suggest alterations in the hydrogen proton state.

Specifically, as shown in Table 1, the relaxation time of free hydrogen in the hydrogel systems decreased from 698.588 ± 0.01 to 329.297 ± 0.15 ms. The smaller the value of T_2 , the greater the binding capacity and the lower the mobility of hydrogen protons in the systems. This proved that the addition of glycerol gradually changed the hydrogen proton state within the gelatin-based hydrogels to intermediate and bound hydrogen.^[31] P_{2b} , P_{21} , and P_{22} are the corresponding area fractions of T_{2b} , T_{21} , and T_{22} , which were directly proportional to the amount of hydrogen protons. Table 1 shows that the proportion of P_{22} was the highest in all gel samples ($> \approx 96\%$), which meant that the free hydrogen was the dominant form of protons present in the hydrogel systems. However, as the time of glycerol substitution increased, P_{22} of the gel decreased and P_{21} and P_{2b} increased. This can be attributed to the fact that the hydrogen bonding of glycerol and gelatin enhanced the gel structure so that the hydrogen protons can be more firmly confined in the network. In summary, the interactions within the gel were consistent with

the results of the microstructural changes inferring that hydrogen bonding between glycerol molecules and gelatin molecules led to the formation of a dense gel 3D network structure (Figure 1f).

2.2. Effect of Oil Droplets on the Properties of Emulsion-Filled Gels with/without Glycerol

Having understood the interaction of glycerol with gelatin, it was important to first ask whether dispersed phase volume fraction would influence the structure and lubrication performance of emulsion-filled gelatin gels. Emulsified oil droplets with different contents (10–30 wt%) were filled into the continuous hydrogel network (named as 0, 10, 20, 30 wt%) and the gel network was modified with an immersion in glycerol for 1 h (named as 0, 10, 20, 30 wt%G).

Figure 2 shows the particle size and distribution of the emulsion-filled gel system before and after replacement. The average droplet size ($D_{4,3}$) of the oil droplets decreased slightly as the oil-phase content increased (Figure 2a). The particle size of the 10 wt% oil droplets was $7.95 \pm 0.07 \mu\text{m}$, and that of the 30 wt% oil droplets was $5.29 \pm 1.03 \mu\text{m}$. This result was confirmed by the shift of the peaks of the particle size distribution to the left in Figure 2b,d. More oil droplets led to an increase in the proportion of gelatin in the system that carried out the role of

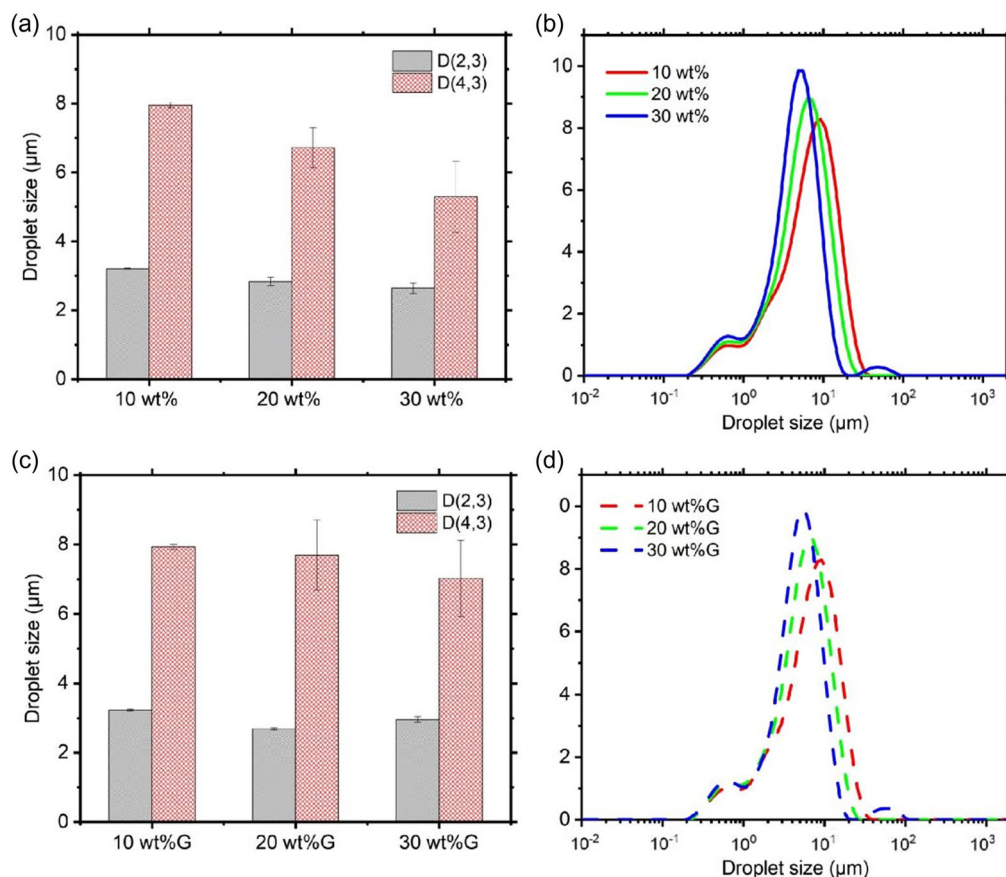


Figure 2. Mean droplet size, a) without glycerol and b) with glycerol, and mean droplet size distribution, c) without glycerol and d) with glycerol, of oil droplets in emulsion-filled gelatin gels coating 10–30 wt% oil. Error bars in (a) and (c) represent standard deviation of three experiments on triplicate samples ($n = 3 \times 3$).

interfacial emulsification. The electrostatic interactions between the gelatin at the droplet surface caused the emulsified oil droplets to repel each other, hindering the aggregation of oil droplets.^[34] Comparing Figure 2c and a, it can be seen that glycerol had little effect on the oil droplet particle size of the system, both which remained within the range of 6–8 μm .

Confocal microstructural observation showed that the spherical emulsified oil droplets were embedded in the green colored, gelatin-based 3D network structure, which proved that the emulsion-filled gel contained either oil-in-water (10–30 wt%) or water/glycerol-in-oil type (10–30 wt%G) (Figure 3) droplets. In the 10 wt% sample, it can be seen that the red oil droplets were encapsulated by gelatin (depicted as green), which indicated that part of the gelatin was adsorbed on the surface of the oil droplets.^[34] Moreover, the oil droplets in the samples with lower volume fraction of dispersed phase (10 wt%/10 wt%G) were not uniformly distributed and were weakly connected with each other. As the number of oil droplets increased, the possibility of their contact with each other increased, and both oil–oil and oil–gel matrix interactions were enhanced.^[35] In contrast, oil droplets in systems with high dispersed volume fraction demonstrated strong inter-droplet interactions. We previously observed similar findings in the emulsion-filled gel system of whey isolate protein.^[19] In addition, comparing the CLSM of the gel system before (top) and after (bottom) replacement, the size of the emulsified droplets did not change significantly (Figure 3). It suggests that glycerol replacement did not have a direct effect on the size of emulsified droplets, which was consistent with the results of sizing (Figure 2). However, the position of the oil droplets may be slightly changed by the entry of glycerol. Oil flocs were apparent in 20 wt%G after substitution (Figure 3). This suggests that the hydrogen bonding of gelatin by glycerol (Figure 1) resulted in more interactions within oil droplets in proximity resulting in enhanced flocculation.^[23,36]

Changes in the microstructure of emulsion-filled gels directly affected their viscoelastic behavior. Figure 4a,b reflects the temperature responsiveness of gels with different oil contents before and after replacement of the continuous phase by glycerol. The storage modulus (G') of all gel systems decreased with increasing temperature.^[37,38] Of more importance, the gel system after substitution had a smoother heating profile and the decrease of G' was delayed. Moreover, we observed that the replaced gels with high oil-phase content were in a molten state (high viscosity, low fluidity) at 37 $^{\circ}\text{C}$, which was between a solution and a gel (Figure 4b). In contrast, the non-displaced gel samples melted into a homogeneous emulsion at 37 $^{\circ}\text{C}$ (Figure 4a). This indicated that the addition of glycerol significantly affected the thermoresponsiveness of the gel system.^[14] Conventional gelatin hydrogels melt easily on heating, leading to disruption of the physical cross-linking network. However, the abundance of hydrogen bonds brought by incorporation of glycerol molecules (Figure 1) enhanced the thermal stability of the physical cross linking, which was attributed to the fact that more energy was required for the breakdown of the hydrogen bonds.^[39]

We then analyzed the rheological behavior of the emulsion-filled gels after replacement. Figure 4c shows that the viscoelasticity of the gel in the linear viscoelastic region (LVER) does not change with strain. However, post LVER, the G' of the emulsion gel decreased rapidly, indicating that the elastic network structure of the gel transitioned to a viscous structure ($G'' > G'$).^[40] Moreover, the increase of oil droplet content enhanced the G' of gels. For example, 30 and 0 wt%G samples had a G' of 81,310 and 574 Pa, respectively. The active filled oil droplets acted as “active fillers” and formed a denser network structure, which can better resist the action of stress.^[35] Second, glycerol reduced the intra- and intermolecular forces within the gelatin molecules, thus reducing the degree of curling of the gelatin molecular

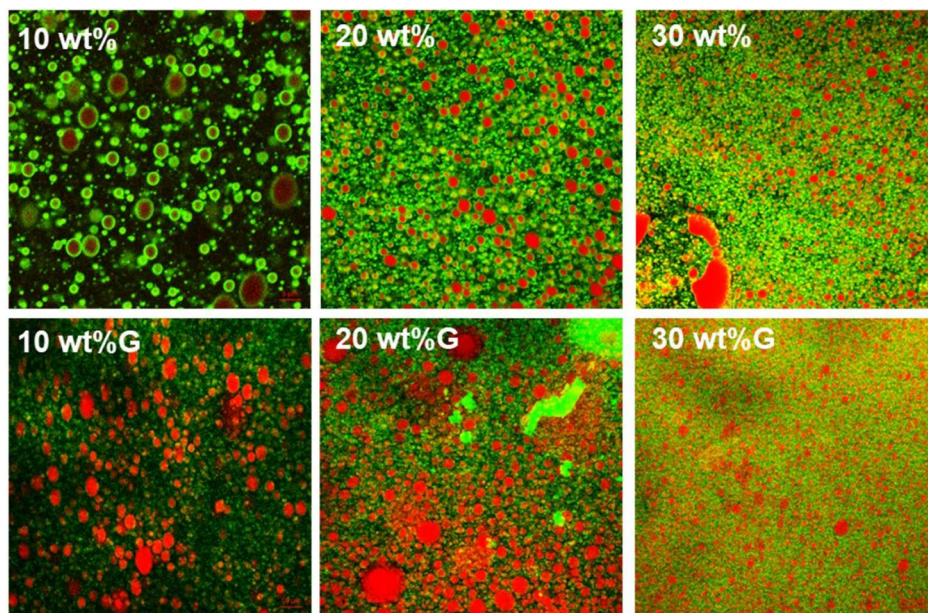


Figure 3. Confocal laser scanning micrographs (CLSMs) of emulsion-filled gels with different oil content (10–30 wt% oil) without (top) or with (bottom) glycerol. Red color represents oil droplets stained by Nile red and green color represents protein stained by fast green.

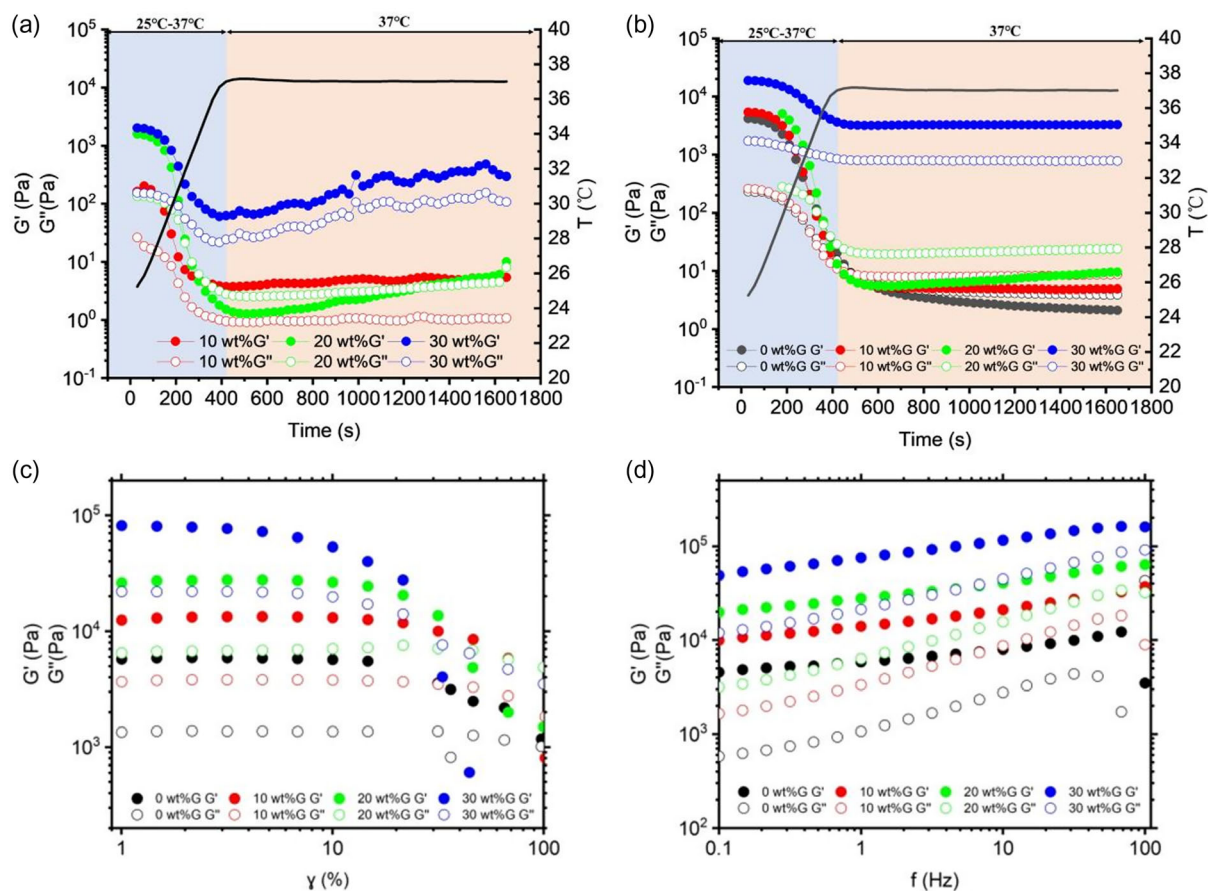


Figure 4. Storage modulus (G' , closed symbols) and loss modulus (G'' , open symbols) of emulsion-filled gelatin gels with different oil content (10–30 wt% oil) with or without added glycerol. Temperature sweep of emulsion-filled gelatin gels a) without glycerol and b) with glycerol, c) strain (γ) sweep, and d) frequency (f) sweep of emulsion-filled gels with glycerol. Values are expressed as means and standard deviations of three measurements on triplicate samples ($n = 3 \times 3$).

chains. The more ordered spatial network structure formed internally also improved the elasticity of the emulsion-filled gelatin gel.^[41,42] In the frequency sweep test, the samples exhibited the typical gel behavior of $G' > G''$ (Figure 4d). The frequency dependence of G' for all samples suggested that the gel network was composed of non-covalent cross links (e.g., hydrogen bonding and hydrophobic interactions).^[43] Similar results were found in the study by Zhou et al. (2018) where weak and brittle water-based gelatin hydrogels turned into glycerol-based organohydrogels with significantly enhanced mechanical properties.^[14]

2.3. Effect of Sugar Alcohols and Oil Droplets on the Lubrication Properties of Emulsion Gel Systems

To establish a link between the lubricating properties of multicomponent emulsion-filled gels and their composition and structures, we further investigated the contribution of each component of the gel to its lubricating properties. We used polydimethylsiloxane (PDMS) contact surfaces to fully examine the tribological behavior of emulsion-filled gels with different oil droplet contents before and after displacement at 37 °C.

2.3.1. Role of Oil Volume Fraction

Figure 5a shows the friction coefficients as a function of entrainment speeds for gelatin-based emulsion-filled gels with different oil droplet contents before displacement by glycerol. All samples showed a similar trend: the friction coefficient (μ) initially remained stable and decreased with increasing entrainment speed, reaching a minimum value before increasing again in the hydrodynamic regimes. For example, μ for the 0 wt% sample (pure gelatin hydrogels) was initially 0.296 ($\bar{U} = 1 \text{ mm s}^{-1}$), then decreased to 0.003 ($\bar{U} = 65 \text{ mm s}^{-1}$), and finally increased again to 0.084 ($\bar{U} = 1000 \text{ mm s}^{-1}$). The μ in the boundary regime at low entrainment speed was almost speed independent (Figure 5a). At this point, there was no fluid dynamic pressure at the contact surface and the friction depended mainly on the interfacial film properties at this molecular length scale. As the entrainment speed increased, the sample shifts toward the mixed lubrication regime. The entrainment of the gel system into the contact surface caused the two surfaces to start separating from each other and the friction coefficient decreased significantly. Finally, at high entrainment speed, the contact surfaces were completely separated. At this point, the fluid viscosity of the

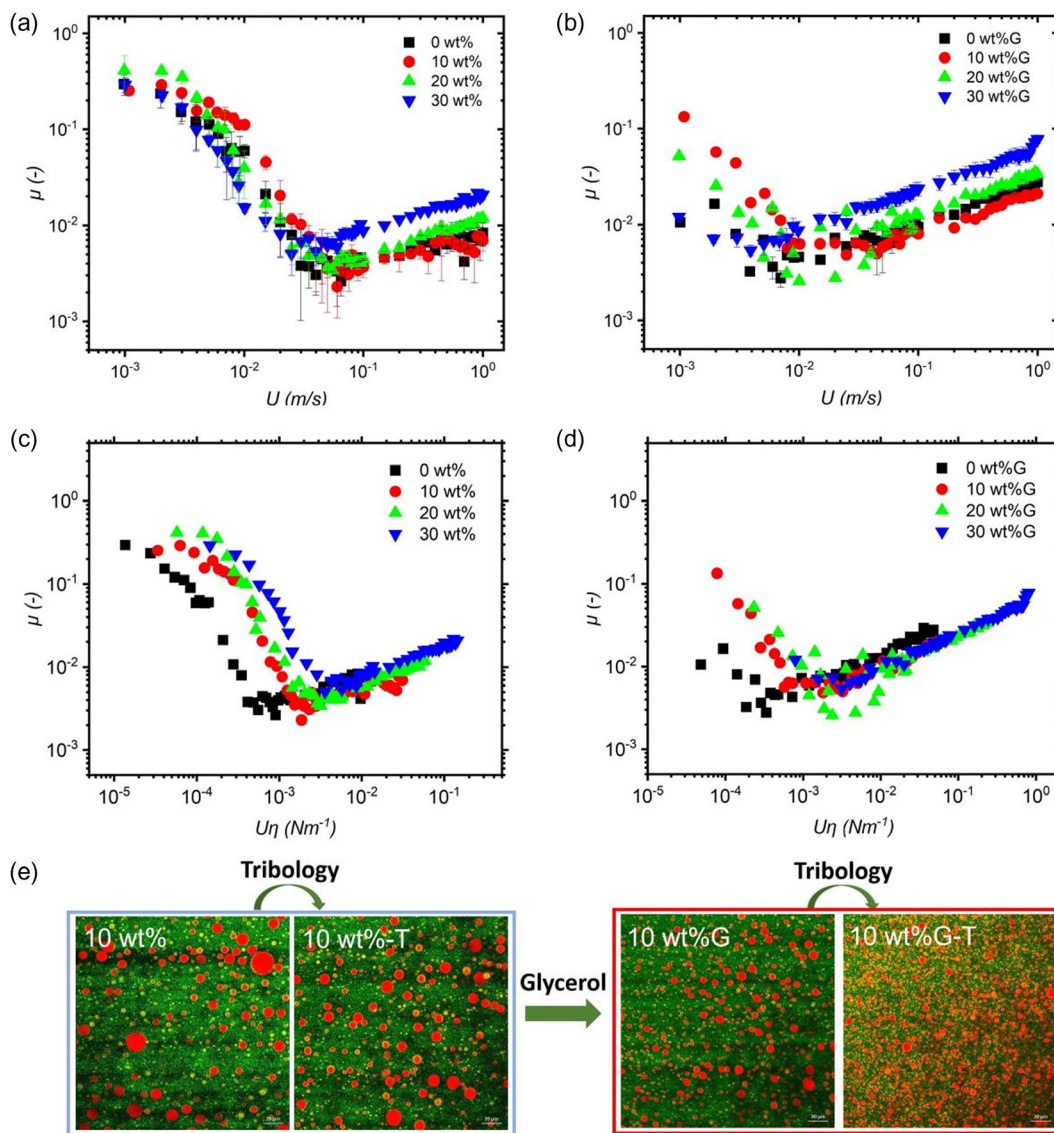


Figure 5. Mean coefficient of friction (μ) of emulsion-filled gels a) without glycerol and b) with glycerol as a function of entrainment speeds (U); scaling of friction data of emulsion-filled gels c) without glycerol and d) with glycerol to viscosity (η) and presenting as a function of $U\eta$; e) the CLSM images of the 10 wt% and 10 wt%G before and after friction test (–T). Error bars in (a) and (b) represent standard deviation of three experiments on triplicate samples ($n = 3 \times 3$).

gel system became the key factor influencing the friction (Figure 7).^[10,11,44–46] Moreover, the friction coefficient of 0 wt% (pure gelatin hydrogels) was lower than that of water at lower entrainment speed (Figure S1, Supporting Information). Since the 0 wt% samples contained only gelatin, this suggested that the frictional behavior of the gel system was mainly determined by the gelatin matrix. Melted gelatin formed an interfacial film between the ball discs of PDMS reducing frictional dissipation.^[47]

We found that the presence of oil droplets in the gel matrix also affected the lubrication behavior of the gel (Figure 5a). Surprisingly, increasing the oil droplet content from 0 to 30 wt% resulted in a significantly higher friction coefficient of the gel system in the hydrodynamic regime (Figure 5a).

The friction coefficients were ≈ 0.084 for the 0 wt% sample and 0.021 for the 30 wt% sample when the entrainment speed was 1000 mm s^{-1} . The oil droplets acting as “active fillers” led to an increase in gel densities and effective viscosity. This was evidenced by the viscosity of the sample in Figure S2a, Supporting Information (30 wt% > 20 wt% > 10 wt% > 0 wt%). In contrast, Saavedra Isusi et al. (2023) found that there was no significant effect of active fillers on the frictional properties of soy protein gel system.^[48] This suggests that in addition to the oil droplet content, the oil droplet clustering was also an important factor influencing the lubrication properties of the gel.

Wijk and Prinz (2005) suggested that high droplet concentration would reduce the friction induced by semisolid products.^[49] However, in our system, it was observed that high oil droplet

content of 30 wt% did lower friction. This may be due to the fact that the gelatin 3D network built a spatial protective layer around the droplets, and were not forming a coalesced tribofilm under tribological stress.^[50] Emulsified systems with complex interfacial microstructures (e.g., Pickering emulsions, emulsion gels, etc.) have been shown to be more resistant to pressure than droplets stabilized with proteins or other surfactants alone.^[51] Hence, preventing oil droplets from spreading and covering the contact surface lead to poor lubrication in the emulsion gels filled with 30 wt% oil droplets.^[52]

To better understand the transition of the samples between different lubrication states, we scaled the μ data to high shear plateau viscosity and plotted μ as a function of entrainment velocity multiplied by the effective viscosity (entrainment speed of 1000 mm s^{-1}) in Figure 5c. It was found that after eliminating the effect of viscosity, gels with high oil droplet content transitioned from the boundary state to the mixed state later (at higher sliding velocities) and had greater coefficients of friction in the boundary and mixed regime. This was due to increased gel interactions and cross linking of the internal network structure, which was detrimental to droplet dispersion at the friction interface. The greater viscosity of the gel network caused them to be more difficult to plate out and entrain in narrow gaps in boundary regime.^[25,45]

De Vicente et al. (2006) found in oil-in-water emulsions that lubrication is determined by the viscosity ratio of the two phases.^[53] If the viscosity of the oil was at least 4 times greater than that of the continuous phase, the oil droplets enter the contact zone and dominate the lubrication properties, otherwise the friction was controlled by the continuous phase. This was in agreement with our results showing that the lubrication behavior of the gel system before replacement was dominated by the continuous phase and influenced by the oil droplet content.

2.3.2. Role of Time and Type of Sugar Alcohol Replacement

Figure 5b shows the Stribeck curves of the gels after glycerol replacement, and they had a similar trend to that of pure glycerol (Figure S2, Supporting Information). Unlike the pre-replacement samples, their Stribeck curves mainly consisted of mixed and hydrodynamic regime with no obvious boundary regimes. The high viscosity of the replaced sample (Figure S2b, Supporting Information) accelerated the onset of mixed regime. This suggested that the substitution of gelatin of glycerol molecules significantly altered the frictional behavior of the emulsion gel system. The reason for the ultralow friction exhibited by the emulsion gel system in the mixed regime after glycerol replacement may be that the hydrogen bonding network formed by the glycerol and gelatin molecules acted as an elastic, lubricating, and hydrated film, which provided repulsive force for the separation of the contact surfaces. Second, the polyhydroxyl structure of glycerol may have had an associative interaction with PDMS, preventing plowing away from the surface. Similar behavior of lower coefficient of friction for PDMS contact was observed by Farias et al. (2020) and Su et al. (2016).^[45,48] They concluded that the surface association of the polymer chains of xanthan gum and polyacrylamide with PDMS enhanced the boundary lubrication properties of the system, respectively. In addition, the increase in friction in the hydrodynamic regime was due to

the increase in viscosity of the gel system caused by glycerol, which formed hydrogen bonds with gelatin molecules for better resistance to shear stress (Figure 1). Second, glycerol itself had a plasticizing effect. Similarly, we compared the difference in conversion between different friction stages of the gel samples after replacement (Figure 5d). The results were similar to the gel samples before replacement; the less viscous samples would enter the hydrodynamic regime earlier.

After the friction test, the microstructural changes of the system were observed, especially the size and distribution of the filled oil droplets. Figure 5e shows the CLSM images of the samples before and after subjecting the samples to tribological stresses. It was observed that the number of oil droplets increased, and the distribution became more uniform. This phenomenon was more obvious in the gel system after replacement (10 wt% G–T). This is due to the fact that hydrogen bonding in the continuous phase significantly enhances the physical cross-linking density within the system hindering the aggregation of oil droplets. At the same time, hydrogen bonding between glycerol and gelatin molecules at the interface ensured the stability of the emulsified oil droplets.

In view of the excellent lubricating properties that glycerol substitution brings to gel systems, a more comprehensive understanding seemed necessary. We compared the differences in lubrication properties of emulsion-filled gel samples containing 20 wt% oil obtained under different substitution times (0–2 h) and different sugar alcohol types (glycerol, sorbitol, xylitol, maltitol). Figure 6a shows that as the glycerol replacement time increased, the friction in the boundary and mixed regime of the gel system decreased significantly, and the friction in the hydrodynamic regime matched with the increased viscosity (Figure S3, Supporting Information). The higher the glycerol content, the more glycerol molecules were adsorbed on the contact surface at low entrainment velocities. In Figure 6b, it can be observed that different sugar alcohols do not have a significant effect on the coefficient of friction of the gel system. Glycerol (C3), sorbitol (C4), xylitol (C5), and maltitol (C12) all contain multiple hydroxyl groups. Although hydroxyl groups play an important role in the lubricating properties of sugar alcohols, the number of hydroxyl groups in individual sugar alcohol molecules may not be responsible for the ultralow friction. In conclusion, the increase of the total sugar alcohol content in the system plays a dominant role in the boundary lubrication process of the gel system, while the number of hydroxyl groups of the sugar alcohol molecules does not have a significant effect.

Figure 7 demonstrates the mechanisms by which solvent displacement (continuous phase) by sugar alcohols and emulsion oil droplets (dispersed phase) affect the lubrication behavior of the emulsion gels. At low entrainment speeds, the emulsion gels containing glycerol (after displacement) had lower friction coefficients, which was attributed to the lubricating film between the PDMS contact surfaces formed by the glycerol molecules. In addition, longer replacement time enhanced the thermal stability of the emulsion gels and hindered the spreading of the molten gel system at the interface, thus affecting the lubricity in the boundary regime. In contrast, at high entrainment speeds, the solvent substitution elevated the viscosity of the emulsion gels leading to the increase of friction coefficient. Here, the oil volume fraction had no direct effect on the friction in the boundary

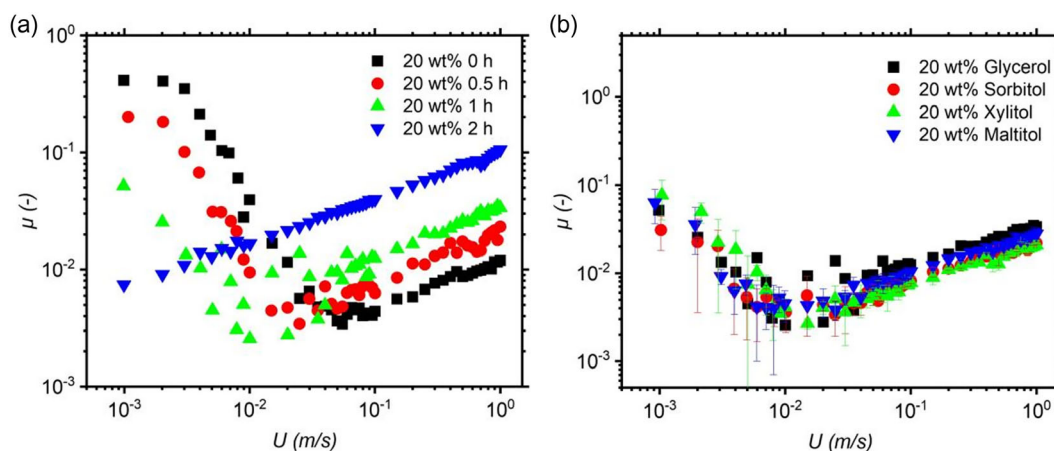


Figure 6. a) Mean coefficient of friction (μ) of 20 wt% oil-containing emulsion-filled gels with different replacement time and b) different types of sugar alcohols, i.e., glycerol, sorbitol, xylitol, and maltitol as a function of entrainment speeds (U). Error bars in (a) and (b) represent standard deviation of three experiments on triplicate samples ($n = 3 \times 3$).

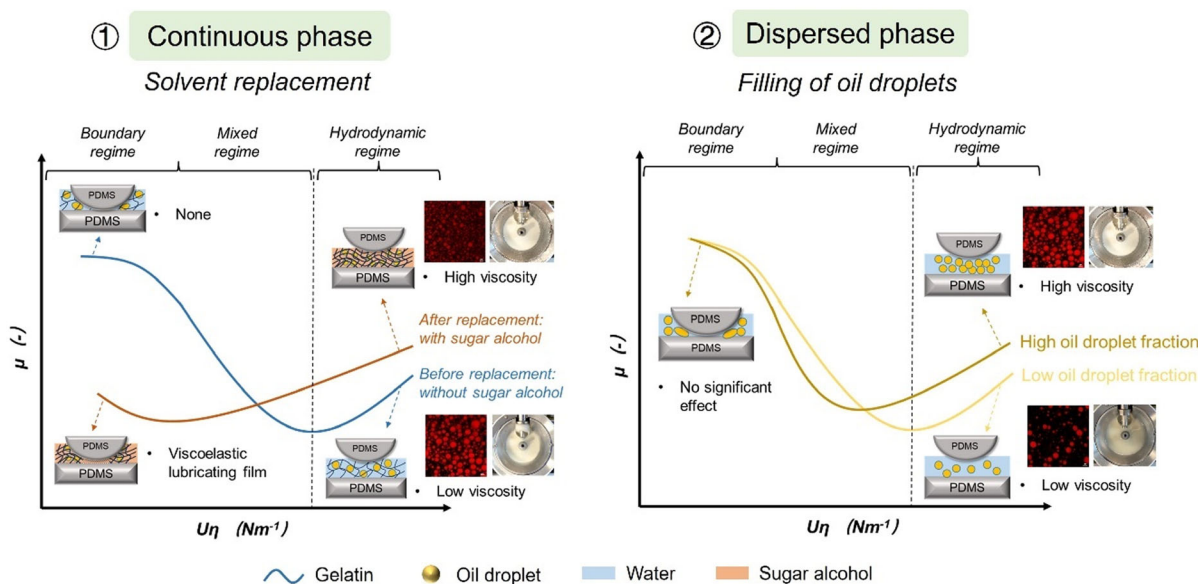


Figure 7. Schematic diagram of the mechanism of glycerol and filled oil droplets driving the lubricating performance of the emulsion-filled gels system.

regime, but significantly affected the lubrication properties in the hydrodynamic regime.

Based on the high lubrication performance at 37 °C, the emulsion gel system in this study shows promise in oral care applications. People with dry mouth syndrome lack natural saliva, which can limit the lubrication of the oral surface. It is now well acknowledged in literature that advanced engineered hydrogel systems may offer significantly enhanced lubricity and address dry mouth conditions by providing the much needed sustained coating.^[9] Pabois et al.^[54] used a variety of microgel-reinforced hydrogels to improve its boundary lubrication efficiency by 41%–99%. Hu et al.^[9] developed a biological lubricant consisting of lactoferrin microgels dispersed in κ -carrageenan hydrogel. These lubricant gels engineered using biocompatible and

biodegradable materials exhibited greater lubricity than real human saliva under different oral simulation conditions. Above and beyond what is reported in the literature, the emulsion gels containing glycerol in this study showing lowering of friction coefficients in the boundary lubrication regimes serve as unique templates to not only lower friction but also may be used to deliver hydrophobic actives through encapsulation in the dispersed droplets, which needs further research attention.

3. Conclusions

In this study, gelatin-based emulsion-filled gels regulated by sugar alcohols and effects of such sugar alcohols (glycerol as

an example) and oil-phase content on the structural properties and lubrication behavior of the gel systems were investigated. The polyhydroxy structure of glycerol reinforced the gelatin gels, enhancing the formation of intermolecular hydrogen bonds with gelatin. The number of hydrogen bonds in the gel systems increased with the increase in glycerol replacement time, which led to greater gel strength. The presence of emulsion oil droplets further made the gel network denser; the former acted as active fillers. Both replacement of continuous phase by sugar alcohols and addition of oil droplets in the dispersed phase can reduce the thermoresponsiveness of otherwise phase-changing, emulsion-filled gelatin gel systems. Tribological results schematically indicated that the adsorbed glycerol formed a lubricating film that could greatly reduce the friction between hydrophobic surfaces in the boundary and mixed regimes. This process was inversely proportional to the replacement time of the glycerol but was independent of the type of sugar alcohols. In the hydrodynamic regime, the samples with higher shear viscosity had larger friction coefficients, which were regulated by the oil droplet volume fraction. This study thus offers new insights into lubrication mechanism of complex hydrogel systems by bringing the dual benefits of reinforcement and lubrication by subtle interplay of oil content and sugar alcohols. The findings will inspire designing hydrogel systems of optimized elasticity with high lubricating properties for food, biomedical, and allied soft matter applications. Ongoing studies are focusing on long-term aging applications of these emulsion-filled hydrogels.

4. Experimental Section

Materials: Gelatin (from pig skin, bloom 180 g, food grade, type A) was provided by Gebeida Co., Ltd. (Hebei, China). Corn oil was supplied by Changshouhua Food Co., Ltd. (Shandong, China). Glycerol (AR grade, 99%) was purchased from Macklin Biochemical Co., Ltd. (Shanghai, China). Sorbitol, xylitol, and maltitol (food grade) were obtained from Puresweet Co., Ltd. (London, UK). Nile red and fast green were products of Sigma-Aldrich (Dorset, UK). All chemicals were of analytical grades unless otherwise specified. MilliQ water purified using Milli-Q apparatus (Millipore, Bedford, UK), with an electrical resistivity not less than 18.2 M Ω cm was used as the solvent.

Preparation of Gelatin-Based Hydrogels: The preparation method of gelatin-based hydrogels was based on a previous study by Zhou et al. (2018) and Sarkar et al. (2015) with slight modifications.^[14,55] An amount of 10 wt% of gelatin was dissolved in MilliQ water by stirring for 30 min at 50 °C. After complete dissolution, the gelatin solution was poured into a plastic petri dish and kept at 4 °C for 1 h to obtain gelatin-based hydrogels. For the samples containing gelatin, the hydrogel was then immersed in glycerol (8 \times weight of the hydrogel) at 25 °C for 0, 0.5, 1, and 2 h to induce the replacement of water. The displaced gel was removed from the container and the excess glycerol was wiped off the surface by filter paper.

LF-NMR: The state of hydrogen protons in gelatin hydrogels with/without glycerol was analyzed using a LF-NMR analyzer (VTNMR20-010 V-I, Niumag, China) to detect the transverse spin-spin relaxation time (T_2) and MRI according to the method of Hou et al. (2022).^[56] Nearly, 2 g of the hydrogel was placed in a cylindrical NMR glass tube (15 mm diameter) and tested by the Carr-Purcell Meiboom-Gill (CPMG) sequence. The test parameters were as follows: spectral width = 100 kHz, number of echoes = 18 000, relaxation decay time = 1.5 ms, number of repeat scans = 4, and repeat interval = 3000 ms. All measurements were repeated three times and the corresponding data were inverted using MultiExp Inv analysis software (Niumag, Shanghai, China).

The MRI of the gels was performed by spin-echo sequences. The test parameters were as follows: repetition time = 500 ms; echo time = 20 ms; slice gap = 1.0 mm; number of slices = 3; and slice width = 2.0 mm. Finally, the middle layer of the samples was taken for uniform mapping and pseudo-coloring.

FTIR Spectroscopy: Molecular interactions within the gelatin hydrogels during glycerol substitution were analyzed by FTIR spectrometer (Spectrum 100, PerkinElmer, UK). The lyophilized samples were mixed with KBr powder and pressed into tablets. The resolution of the test was 4 cm⁻¹ and the scanning range was 4000–400 cm⁻¹ with 64 scans. The peak values were calculated using Thermo Scientific OMNIC software (Thermo Fisher Scientific Inc., USA).

Cryo-SEM: The microstructure of the gelatin hydrogels was observed by a Cryo-SEM (SU8010, Hitachi, Japan).^[40,57] Samples were frozen by immersion in liquid nitrogen at -170 °C and then transferred to a cryo-preparation chamber (PP3000T, Quorum Inc., UK) for crosscutting. Samples were gold sprayed after sublimation at -75 °C for 30 min. Finally, the samples were imaged in the observation chamber at a voltage of 10.0 kV.

Preparation of Gelatin-Based Emulsion-Filled Gels with/without Glycerol: Primary emulsions were prepared by shearing 5 wt% aqueous gelatin solution and 0, 10, 20, and 30 wt% of corn oil through a high-speed blender (T18 digital ULTRA-TURRAX, IKA, Germany) at 11 000 rpm for 3 min. The obtained primary emulsion was slowly poured into 5 wt% aqueous gelatin solution and stirred at 50 °C for 15 min. The gelatin content of the final emulsion system was 10 wt%. The final emulsion was poured into a plastic petri dish and kept at 4 °C for 1 h to obtain gelatin-based emulsion-filled gels. These emulsion-filled gels were soaked in glycerol (8 \times weight of the emulsion-filled gelatin gels) for 1 h at 25 °C to obtain the displaced emulsion-filled gels.

To have a more comprehensive understanding of the effect of the replacement time and type of sugar alcohols on the gel properties, we selected 20 wt% of emulsion-filled gels that were replaced in glycerol for 0, 0.5, 1, and 2 h, and in glycerol, sorbitol, xylitol, and maltitol for 1 h, respectively.

Droplet Size: The droplet size distribution of emulsions in the emulsion-filled gels was measured using a Malvern MasterSizer 3000 (Malvern Instruments Ltd., Malvern, Worcestershire, UK). An amount of 1 g of the gel was dissolved in MilliQ water and diluted at a 0.01 wt% droplet concentration. The refractive coefficients of the oil and protein were set to 1.470 and 1.330, respectively. The volume mean diameter of the oil droplets was recorded as D (4,3) and the surface area mean diameter was recorded as D (3,2). Tests were performed at 25 °C for triplicate samples with three measurements.

CLSM: The Zeiss LSM 780 CLSM (Carl Zeiss MicroImaging GmbH, Jena, Germany) was used to observe the microstructure of different emulsion-filled gels with/without glycerol addition. The gelatin and oil in the gels were stained by fast green (1 mg mL⁻¹) and Nile red (1 mg mL⁻¹), respectively. The dyed samples were placed on glass slides and secured with a glass coverslip. They were imaged using an oil immersion 63 \times lens under Ar laser (488 nm) and HeNe laser (633 nm) excitation light.

Rheological Measurement: A controlled stress rheometer (Kinexus Ultra+, Malvern Instruments Ltd., Worcestershire, UK) equipped with a steel parallel plate (40 mm diameter and 1 mm gap) was used to evaluate the viscoelastic properties of emulsion-filled gels. All samples were equilibrated for 2 min before measurements and covered with a thin layer of silicone oil to prevent the water evaporation. 1) Apparent viscosity: the viscosity (η) of emulsions was tested from 0.1 to 1000 s⁻¹ at 37 °C. 2) Temperature sweep: the thermal responsiveness of gels was measured by temperature sweep. The temperature was increased from 25 to 37 °C at a fixed rate of 5 °C min⁻¹, and then maintained at 37 °C for 20 min (frequency = 1 Hz; strain = 0.1%). 3) Strain sweep: the LVER of emulsion-filled gels was determined by strain sweep (0.1%–100%) at 25 °C (frequency = 1 Hz). 4) Frequency sweep: frequency sweep was conducted at 0.1–100 Hz at 25 °C (strain = 0.1%).

Tribological Measurement: Tribological properties of the samples were measured using a mini-traction machine (PCS Instruments, UK) equipped with PDMS ball-on-disc tribopairs.^[58] Commercially available PDMS balls

(19 mm diameter) and discs (46 mm diameter, 4 mm thickness) were purchased from PCS Instruments, UK. The test parameters were as follows: slide-to-roll ratio of 50%; entrainment speed (U) of 1–1000 mm s⁻¹; temperature of 37 °C; and load of 2.0 N. The variation of coefficient of friction (μ) was plotted as a function of entrainment speed (U) or scaled to high shear plateau viscosity (η_{1000}) at the limiting high shear rate ($\dot{\gamma} = 1000 \text{ s}^{-1}$).^[10] In addition, the microstructural changes of the samples before and after friction were observed using CLSM.

Statistical Analysis: All measurements were repeated three times, unless otherwise stated. The mean and standard deviation data were analyzed by Origin Pro 2021 using triplicate measurements. One-way analysis of variance was conducted by SPSS 20.0 to determine the significant differences between the mean values with a significance level of $p < 0.05$.

Supporting Information

Supporting Information is available from the Wiley Online Library or from the author.

Acknowledgements

This research was funded by National Natural Science Foundation of China (grant no. 31972073) and the China Scholarship Council (grant no. 202206350065). The authors AAC and AS acknowledge funding received from EAT4AGE project from (Biotechnology and Biological Sciences Research Council [BBSRC], UK) under the umbrella of the European Joint Programming Initiative “A Healthy Diet for a Healthy Life” (JPI HDHL) and of the ERA-NET Cofund ERA-HDHL (GA N°696295 of the EU Horizon 2020 Research and Innovation Programme).

Conflict of Interest

The authors declare no conflict of interest.

Data Availability Statement

The data that support the findings of this study are available from the corresponding author upon reasonable request.

Keywords

active fillers, emulsion, glycerol, hydrogel, rheology, tribology

Received: January 17, 2024

Revised: May 17, 2024

Published online: June 7, 2024

- [1] Z. Zhang, J. Hao, *Adv. Colloid Interfac.* **2021**, 292, 102408.
- [2] L. T. Mashabela, M. M. Maboja, N. F. Miya, T. O. Ajayi, R. S. Chasara, M. Milne, M. S. Poka, *Gels* **2022**, 9, 563.
- [3] H. Khalesi, W. Lu, K. Nishinari, Y. Fang, *Adv. Colloid Interfac.* **2020**, 285, 102278.
- [4] T. Zhu, Y. Ni, G. M. Biesold, Y. Cheng, M. Ge, H. Li, Y. Lai, *Chem. Soc. Rev.* **2023**, 52, 473.
- [5] Z. Zeng, M. Zhu, L. Chen, Y. Zhang, T. Lu, Y. Deng, R. Xiong, *Compos. Part B-Eng.* **2022**, 247, 110313.
- [6] D. Li, W. Zhan, W. Zuo, L. Li, J. Zhang, G. Cai, Y. Tian, *Chem. Eng. J.* **2022**, 450, 138417.
- [7] X. Liu, J. Liu, S. Lin, X. Zhao, *Mater. Today* **2020**, 36, 102.
- [8] A. Sarkar, S. Soltanahmadi, J. Chen, J. R. Stokes, *Food Hydrocolloid.* **2021**, 117, 106635.
- [9] J. Hu, E. Andablo-Reyes, S. Soltanahmadi, A. Sarkar, *ACS Macro Lett.* **2020**, 9, 1726.
- [10] S. Soltanahmadi, B. S. Murray, A. Sarkar, *Food Hydrocolloid.* **2022**, 129, 107660.
- [11] N. Yang, Y. Feng, C. Su, Q. Wang, Y. Zhang, Y. Wei, Y. Fang, *Food Hydrocolloid.* **2020**, 107, 105945.
- [12] O. Torres, E. Andablo-Reyes, B. Murray, A. Sarkar, *Acs Appl. Mater. Inter.* **2018**, 10, 26893.
- [13] F. Chen, D. Zhou, J. Wang, T. Li, X. Zhou, T. Gan, X. Zhou, *Angew. Chem.* **2018**, 130, 6678.
- [14] D. Zhou, F. Chen, J. Wang, T. Li, B. Li, J. Zhang, X. Zhou, *J. Mater. Chem.* **2018**, 6, 7366.
- [15] Q. Zeng, *J. Adhes. Sci. Technol.* **2018**, 32, 1911.
- [16] J. Li, C. Zhang, M. Deng, J. Luo, *RSC Adv.* **2015**, 5, 30861.
- [17] J. Li, C. Zhang, J. Luo, *Langmuir* **2011**, 27, 9413.
- [18] C. Matta, L. Joly-Pottuz, M. D. B. Bouchet, J. M. Martin, M. Kano, Q. Zhang, W. A. Goddard III, *Phys. Rev. B* **2008**, 78, 085436.
- [19] Y. Lu, L. Mao, M. Cui, F. Yuan, Y. Gao, *J. Agr. Food Chem.* **2019**, 67, 6466.
- [20] L. Bai, S. Huan, O. J. Rojas, D. J. McClements, *J. Agr. Food Chem.* **2021**, 69, 8944.
- [21] X. Li, W. Chen, J. Hao, D. Xu, *Colloid. Surface. A* **2023**, 665, 131238.
- [22] K. Liu, M. Stieger, E. van der Linden, F. van de Velde, *Food Hydrocolloid.* **2015**, 44, 244.
- [23] P. L. Fuhrmann, G. Sala, E. Scholten, M. Stieger, *Food Hydrocolloid.* **2020**, 105, 105856.
- [24] A. Chojnicka, G. Sala, C. G. De Kruijff, F. Van de Velde, *Food hydrocolloid.* **2009**, 23, 1038.
- [25] S. Mu, F. Ren, Q. Shen, H. Zhou, J. Luo, *Food Hydrocolloid.* **2022**, 131, 107754.
- [26] J. Yang, Z. Gu, L. Cheng, Z. Li, C. Li, X. Ban, Y. Hong, *Carbohydr. Polym.* **2021**, 262, 117926.
- [27] J. Skopinska-Wisniewska, M. Tuszynska, E. Olewnik-Kruszkowska, *Mater.* **2021**, 14, 396.
- [28] M. S. Hoque, S. Benjakul, T. Prodpran, *Food Hydrocolloid.* **2011**, 25, 1085.
- [29] M. Ahmad, S. Benjakul, *Food Hydrocolloid.* **2011**, 25, 381.
- [30] X. Shu, Y. Wei, X. Luo, J. Liu, L. Mao, F. Yuan, Y. Gao, *Food Hydrocolloid.* **2023**, 134, 108088.
- [31] K. C. Yang, C. C. Wu, Y. H. Cheng, T. F. Kuo, F. H. Lin, *Transpl. P.* **2008**, 40, 3623.
- [32] B. Panchal, T. Truong, S. Prakash, N. Bansal, B. Bhandari, *Food Chem.* **2020**, 333, 127538.
- [33] R. Coronado, S. Pekerar, A. T. Lorenzo, M. A. Sabino, *Polym. Bull.* **2011**, 67, 101.
- [34] P. L. Fuhrmann, G. Sala, M. Stieger, E. Scholten, *Food Res. Int.* **2019**, 122, 537.
- [35] D. J. McClements, *Curr. Opin. Colloid In.* **2012**, 17, 235.
- [36] P. L. Fuhrmann, S. Breunig, G. Sala, L. Sagis, M. Stieger, E. Scholten, *J. Colloid Interf. Sci.* **2022**, 607, 389.
- [37] J. Yan, S. Li, G. Chen, C. Ma, D. J. McClements, X. Liu, F. Liu, *Food Hydrocolloid.* **2023**, 137, 108384.
- [38] M. Djaborov, P. Papon, *Polym* **1983**, 24, 537.
- [39] F. M. Vanin, P. J. D. A. Sobral, F. C. Menegalli, R. A. Carvalho, A. M. Q. B. Habitante, *Food Hydrocolloid.* **2005**, 19, 899.
- [40] Y. Lu, R. Zhang, Y. Jia, Y. Gao, L. Mao, *Food Hydrocolloid.* **2023**, 139, 108563.7.
- [41] M. Thomazine, R. A. Carvalho, P. J. Sobral, *J. Food Sci.* **2005**, 70, E172.
- [42] D. Hardman, T. George Thuruthel, F. Iida, *Npg Asia Mater.* **2022**, 14, 11.
- [43] S. B. Ross-Murphy, *Polym. Gels Netw.* **1994**, 2, 229.

- [44] S. Soltanahmadi, M. Wang, M. K. Gul, E. Stribiřcaia, A. Sarkar, *Sustain. Food Proteins* **2023**, 1, 149.
- [45] B. V. Farias, L. C. Hsiao, S. A. Khan, *Acs Appl. Polym. Mater.* **2020**, 2, 1623.
- [46] E. Liams, S. D. Connell, A. Sarkar, *Nanoscale Adv.* **2023**, 5, 1102.
- [47] Z. Pang, Y. Luo, B. Li, M. Zhang, X. Liu, *Food Hydrocolloid.* **2020**, 101, 105558.
- [48] H. Su, X. Wang, M. Du, Y. Song, Q. Zheng, *RSC Adv.* **2016**, 6, 5695.
- [49] R. A. de Wijk, J. F. Prinz, *Food Qual. Prefer.* **2005**, 16, 121.
- [50] M. Anvari, H. S. Joyner, *Food Hydrocolloid.* **2018**, 79, 518.
- [51] X. Feng, H. Dai, L. Ma, Y. Fu, Y. Yu, H. Zhou, Y. Zhang, *Colloid Surface B* **2020**, 196, 111294.
- [52] G. I. Saavedra Isusi, J. Marburger, N. Lohner, U. S. van der Schaaf, *Gels* **2023**, 9, 473.
- [53] J. De Vicente, J. R. Stokes, H. A. Spikes, *Food hydrocolloid.* **2006**, 20, 483.
- [54] O. Pabois, A. Avila-Sierra, M. Ramaioli, M. Mu, Y. Message, K. M. You, A. Sarkar, *Sci. Rep.* **2023**, 13, 19833.
- [55] A. Sarkar, J. M. Juan, E. Kolodziejczyk, S. Acquistapace, L. Donato-Capel, T. J. Wooster, *J. Agr. Food Chem.* **2015**, 63, 8829.
- [56] Y. Hou, H. Liu, D. Zhu, J. Liu, C. Zhang, C. Li, J. Han, *Food Hydrocolloid.* **2022**, 129, 107602.
- [57] A. Araiza-Calahorra, Z. J. Glover, M. Akhtar, A. Sarkar, *Food Hydrocolloid.* **2020**, 105, 105794.
- [58] E. M. Krop, M. M. Hetherington, M. Holmes, S. Miquel, A. Sarkar, *Food Hydrocolloid.* **2019**, 88, 101.